Evaluation of the Severity of Chronic Hepatitis C with 3-T 1H-MR Spectroscopy

Antonio Orlacchio[1]
Francesca Bolacchi[1]
Marcello Cadioli[2]
Alberto Bergamini[3]
Valeria Cozzolino[1]
Mario Angelico[4]
Giovanni Simonetti[1]

OBJECTIVE. The purpose of this study was to compare the spectral characteristics of lipids, choline-containing compounds, and glutamine–glutamate complex assessed with 1H-MR spectroscopy with the histologic findings in patients with chronic hepatitis C.

SUBJECTS AND METHODS. Nine healthy controls and 30 patients with biopsy-proven hepatitis C virus–related liver disease participated in this prospective study. Degree of fibrosis and histologic activity were scored according to the METAVIR classification. The percentage of involved hepatocytes was used to grade steatosis. Hepatic spectra were obtained with a 3-T spectroscopic system. Tenfold cross-validated stepwise discriminant analysis was performed to classify disease severity on the basis of the spectroscopic findings.

RESULTS. There was a strong correlation between 1H-MR spectroscopically measured lipid concentration and the degree of steatosis at histologic examination ($r = 0.9236$, $p < 0.0001$). This finding enabled clear separation of groups according to degree of histologically determined steatosis. Variation in lipid concentration was consistent with the degree of steatosis ($r = 0.7265$, $p < 0.0001$) and stage of fibrosis ($r = 0.8156$, $p < 0.0001$). In univariate analysis, concentrations of both choline-containing compounds and glutamine–glutamate complex had a direct correlation with histologic grade ($p < 0.0001$) and degree of steatosis ($p < 0.0001$) but not with stage of fibrosis ($p > 0.05$). In multivariate analysis, the only factor independently associated with concentrations of choline-containing compounds and glutamine–glutamate complex was histologic grade. In cross-validated discriminant analysis based on choline-containing compound, glutamine–glutamate complex, and lipid resonance, 70% (21 of 30) of the histologic grade groups and 73% (22 of 30) of the steatosis groups were correctly classified.

CONCLUSION. Hydrogen-1 MR spectroscopy can be an alternative to liver biopsy in the evaluation of steatosis and necroinflammatory activity in liver disease but is not useful for complete evaluation of hepatic fibrosis.

There is little doubt that in the assessment of common hepatic diseases, markers are needed that can be measured noninvasively. Several markers have been found useful in this regard, but they are not sufficiently reliable [1–3]. Liver biopsy will continue to be the reference standard in assessment of the severity of diffuse liver disease until noninvasively measured markers are validated and clinically accepted. Several clinical limitations are associated with the use of liver biopsy. It is an invasive and costly procedure prone to complications, some minor, such as pain, others severe, the recorded risk of death being 0.01% [4–6]. Moreover, high sampling variability and high intrapathologist and interpathologist variability have been reported [7–9]. Alternative techniques for assessing the severity of diffuse liver disease are urgently needed.

MR spectroscopy has been found promising. Phosphorus-31 MR spectroscopy has been used to study liver metabolism in vivo [10–12]. Lim and colleagues [10] found that in vivo 31P-MR spectroscopy may be promising in evaluation of the severity of chronic hepatitis C. An important limitation of 31P-MR spectroscopy, however, is that it cannot be used to measure hepatic lipid content, which plays an important pathogenetic role in the development of the inflammation and fibrosis associated with liver disease [13–17]. Unlike 31P-MR spectroscopy, 1H-MR spectroscopy may be accurate for in vivo quantification of liver fat deposition [18, 19]. Cho and colleagues [20] suggested that 1H-MR spectroscopy may have utility in measuring the degree

of fibrosis in patients with chronic hepatitis. To confirm and expand these results, we undertook an in vivo study to compare the [1]H-MR spectral characteristics of lipids, choline-containing compounds, and glutamine–glutamate complex with the histologic features (degree of steatosis, grade of activity, and stage of fibrosis) in patients with chronic hepatitis C. Metabolites were measured at 3 T with respect to intrahepatic water content, the concentration of which remains constant as disease progresses.

Subjects and Methods

Patients

Thirty patients with chronic hepatitis C (17 men, 13 women; mean age, 55 years; range, 28–71 years) were included in the study. Inclusion criteria were the presence of anti–hepatitis C virus (HCV) antibodies detected with a third-generation test, detectable serum HCV RNA, and liver biopsy findings compatible with chronic hepatitis C. Patients with chronic hepatitis B, cirrhosis, or autoimmune hepatitis were excluded. Two patients had a history of drug abuse and two a history of blood transfusion. Liver biopsy was performed within 30 days before or after spectroscopic analysis. At the time of spectroscopic analysis, none of the patients had fever or evidence of other infectious diseases, inflammatory disorders, or malignancy.

A total of nine healthy volunteers who matched the enrolled patients in age and sex acted as controls. All controls had no history of liver disease, alcoholism, blood transfusion, or a positive test result for anti-HCV, anti–hepatitis B virus, or anti-HIV antibodies. All controls had a body mass index (weight in kilograms divided by height squared in meters) less than 27, cholesterol level less than 200 mg/dL, triglyceride level less

than 170 mg/dL, and no evidence of fatty liver at sonography.

The study was approved by our internal committee. All patients and controls gave written informed consent. Quantification of HCV RNA in serum samples was performed with a commercially available kit (Amplicor HCV monitor TM test, Roche Diagnostic Systems). The limit of detection of the HCV RNA assay was fewer than 200 copies/mL. HCV genotype was determined for all patients with a line probe assay (Inno-LiPA HCV II, Innogenetics). Genotypes were classified according to the system of Simmonds and colleagues [21].

Histologic Evaluation

Liver biopsy specimens longer than 10 mm were fixed in formalin, embedded in paraffin, and stained with H and E or picrosirius red for collagen and Perls' technique for iron. All biopsies were performed on the right hepatic lobe, where the sample for MR spectral acquisitions was located. For each liver biopsy specimen, stages of fibrosis and grade of histologic activity (histologic grade) were grouped according to the METAVIR classification [22]. Grades of histologic activity indicating the intensity of necroinflammatory lesions were as follows: 0, no activity; 1, mild activity; 2, moderate activity; 3, severe activity. Fibrosis was staged as follows: 0, no fibrosis; 1, portal fibrosis without septa; 2, few septa; 3, numerous septa without cirrhosis; 4, cirrhosis. Steatosis was graded as follows [23]: 0, none; 1, mild (involving < 10% of hepatocytes); 2, moderate (involving 10–30% of hepatocytes); and 3, severe (involving > 30% of hepatocytes).

MR Spectroscopy

MR spectroscopy was performed with a 3-T system (Achieva, Philips Medical Systems) by a radiologist and a clinical scientist both experienced

with MR spectroscopy. A Q body coil was used for the radiofrequency-transmitting signal and a body surface coil for signal receiving. Spectra were acquired with a 90-180-180 volume-selective single-voxel point-resolved spectroscopic sequence (PRESS) (TR/TE, 1,500/38; 256 measurements; 1,024 sample points yielding an acquisition time of 6:38 minutes). Although a longer TR would minimize T1 weighting in the signal, the chosen TR was an acceptable compromise between the T1 effects and the examination time. A longer TR would have been ideal, but in our clinical setting it would have led to a longer scanning time with the consequent increasing risk of motion artifacts.

The voxel (volume of interest [VOI]) size was 30 × 30 × 40 mm. T2-weighted images were used to locate the voxel deep within the right hepatic lobe to avoid large blood vessels and the gallbladder (point 1) (Fig. 1). To reduce to a minimum respiratory motion–induced magnetic field inhomogeneity and the consequent risk of decrease in sensitivity and precision due to accentuated line-broadening artifacts, patients were trained to perform very relaxed and calm respiration. No outer-volume suppression bands were used because the VOI was carefully located fully inside the deep hepatic parenchyma to prevent contamination by subcutaneous fat and adjacent structures. Fully automated frequency determination, power optimization, and shimming phases were performed in the VOI. Two proton MR spectra were acquired from the same VOI for every case: a water-suppressed PRESS sequence with a selective excitation pulse to crush the water signal and a water-nonsuppressed PRESS sequence without the selective excitation pulse. Because it remains stable during disease progression, water was used as an internal stable standard of reference for metabolite quantification. To assess the reproducibility of the [1]H-MR spectroscopic results, analyses were repeated in triplicate, and results were expressed as the mean of three experiments. Spectroscopy was conducted with the subject in the fasting state.

Processing of Spectral Data

Data were processed with an automatic customized script on the MRI console (Intera 3T, Philips Medical Systems) by a radiologist and a clinical scientist experienced with MR spectroscopy and blinded to the clinical patient data. The script entailed an initial baseline calculation and subtraction with a polynomial function. Metabolites to be estimated were defined with a reference database of known peaks [24]. For water-nonsuppressed acquisition, the water peak was identified and assigned a value of 4.7. For the water-suppressed signal, the metabolite peaks were assigned as
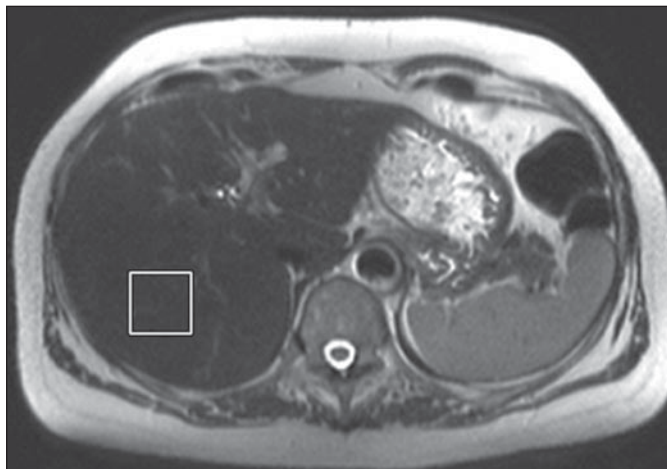

Fig. 1—45-year-old healthy male volunteer. MR image shows voxel positioning.

follows: lipid peak, 0.9–1.2 ppm; glutamate–glutamine complex peak, 2.1–2.4 ppm; choline-containing compound peak, 3.2–3.3 ppm. A gaussian line shape was assumed for fitting of all resonances. The acquired spectra were analyzed with a Marquardt-Levenberg least squares algorithm, in which the differences between the acquired spectra are iteratively minimized and the model-based spectrum are defined a priori on the basis of the database and the gaussian constraint. After the algorithm was applied, the script displayed the estimated peak areas. Resonance areas were normalized by division of each fitted resonance of interest area value in the water-suppressed spectrum by the fitted water area value in the corresponding nonsuppressed water spectrum. The particular metabolite concentration was expressed in relative units according to the following pattern: metabolite/water content = (area of metabolite × 1,000) / area of nonsuppressed water.

Statistical Analysis

Data were analyzed with the nonparametric Mann-Whitney U test. Correlations for the univariate analysis were evaluated with Spearman's nonparametric test. To assess the independent value of each parameter related to choline-containing compounds and glutamine–glutamate complex, multiple regression analysis was performed by means of stepwise logistic regression analysis. A value of $p < 0.05$ was considered significant.

On the basis of the spectroscopic findings, histologic grade and steatosis were classified with 10-fold cross-validated stepwise discriminant analysis. In stepwise discriminant analysis, a model of discrimination is built step by step. Specifically, at each step all variables are reviewed and evaluated to determine which one contributes most to the discrimination between groups. That variable is included in the model, and the process is initiated again. Performance assessment of the discriminant analysis was conducted with 10-fold cross-validation estimation. In the 10-fold cross-validation, the data were divided into 10 subsets (learning samples) of approximately equal size. The analysis was performed 10 times, once for each subset, and each time one patient was left out (test sample). The test sample was in turn classified with the set of discriminant functions derived from the subset analyzed. Classification accuracy was defined as the ratio between the number of cases correctly classified and the total number of cases in the set. All statistical analyses were performed with the statistical package SPSS (version 10.0.1, SPSS) for Microsoft Windows.

Results

Patients

The clinical and histopathologic characteristics are summarized in Table 1.

Correlation Between Water Peak Areas and Histopathologic Findings

We analyzed the correlation between the peak area of nonsuppressed water determined with [1]H-MR spectroscopy and the histopathologic characteristics among patients with hepatitis C. The hepatic content of water did not vary significantly with disease severity. As shown in Figure 2, there was no statistically significant correlation between water content (arbitrary units) and the degree of steatosis, histologic grade, or stage of fibrosis. Thus the relative metabolite-to-water ratios were obtained by dividing the peak areas of lipid, choline-containing compounds, and glutamine–glutamate complex by the peak area of water.

Correlation Between Spectroscopic Features of Lipids and Histopathologic Findings

As shown in Figure 3A, there was a strong direct correlation between [1]H-MR spectroscopically measured lipid concentration and the degree of steatosis at histologic examination ($r = 0.9236$; 95% CI, 0.8411–0.9641; $p < 0.0001$). Figure 3A also shows that measurement of hepatic lipids with [1]H-MR spectroscopy resulted in clear separation between the groups formed according to degree of histologically determined steatosis. Lipid concentration measured with [1]H-MR spectroscopy and histologic grade consistently varied together ($r = 0.7265$; 95% CI, 0.4875–0.8642; $p < 0.0001$). A significant difference in lipid resonance, however, was achieved only between patients with histologic grade 0–1 disease and patients with histologic grade 2–3 disease (Fig. 3B). Similarly, a significant direct correlation was found between [1]H-MR spectroscopically measured lipid concentration and fibrosis score ($r = 0.8156$; 95% CI, 0.6382–0.9108; $p < 0.0001$). Again, a significant difference in lipid resonance was achieved only between patients with fibrosis scores of 0–1 and patients with fibrosis scores of 2–3 (Fig. 3C).

Correlation Between Spectroscopic Features of Choline-Containing Compounds and Glutamine–Glutamate Complex and Histopathologic Findings

An increase in both choline-containing compounds ($r = 0.9166$; 95% CI, 0.8270–0.9607; $p < 0.0001$) and glutamine–glutamate

TABLE 1: Biochemical and Histologic Characteristics

Variable	Age (y)	Sex (M/F)	Serum Hepatitis C Virus RNA (copies/mL × 10^3)	Genotype (1b/not 1b)	Alanine Aminotransferase (mU/mL)[a]
Severity of steatosis					
None ($n = 12$)	54 ± 12	5/7	942 ± 614	9/3	124 ± 72
Mild ($n = 9$)	56 ± 12	6/3	775 ± 539	5/4	139 ± 57
Moderate ($n = 5$)	57 ± 10	3/2	1,313 ± 1,020	4/1	139 ± 63
Severe ($n = 4$)	53 ± 4	3/1	914 ± 314	3/1	164 ± 59
Grade of histologic activity					
0 ($n = 8$)	52 ± 13	4/4	979 ± 766	4/4	76 ± 18
1 ($n = 12$)	56 ± 11	10/2	905 ± 544	8/4	147 ± 46
2 ($n = 5$)	60 ± 6	1/4	931 ± 275	4/1	151 ± 68
3 ($n = 5$)	51 ± 6	2/3	1,091 ± 1,010	5/0	191 ± 79
Stage of fibrosis					
0 ($n = 6$)	54 ± 15	3/3	946 ± 377	2/4	77 ± 22
1 ($n = 14$)	55 ± 11	8/6	1,110 ± 910	11/3	137 ± 50
2 ($n = 7$)	56 ± 8	4/3	954 ± 615	6/1	186 ± 82
3 ($n = 3$)	54 ± 5	2/1	758 ± 508	2/1	137 ± 31

Note—No statistically significant differences were found between [1]H-MR spectroscopically measured concentrations of lipids, choline-containing compounds, and glutamine–glutamate complex and age, sex, hepatitis C virus RNA copies, genotype, or alanine aminotransferase concentration (data not shown).
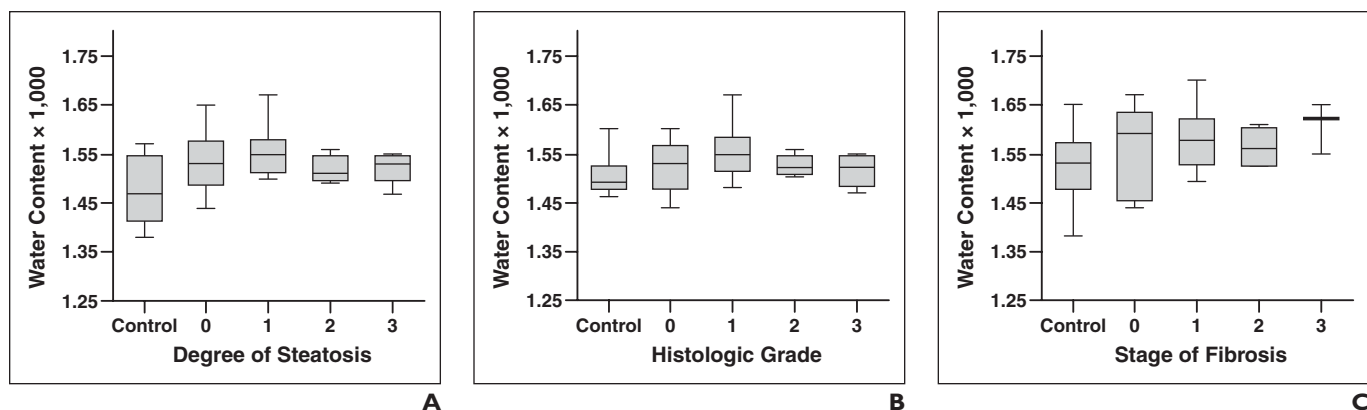
[a]Normal value < 40 mU/mL.

Fig. 2—Correlation between water content and disease severity.
A–C, Graphs show no statistically significant correlation between water content (relative units) and degree of steatosis (**A**), histologic grade (**B**), or fibrosis stage (**C**).
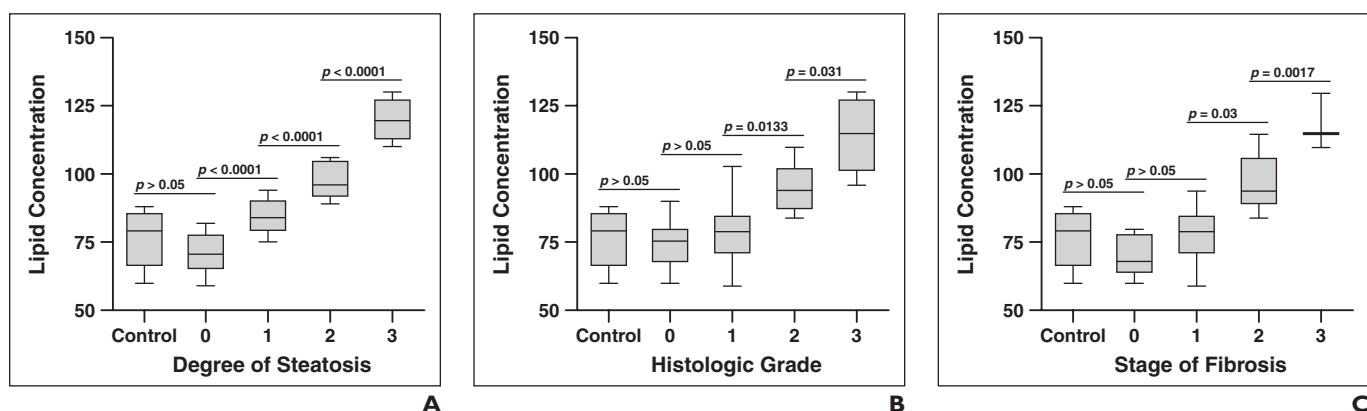

Fig. 3—Correlation between lipid level and disease severity.
A–C, Graphs show elevation of lipid level (relative units) with severity of steatosis with clear separation between all steatosis grades (**A**), between histologic grade 0–1 versus histologic grade 2–3 hepatitis (**B**), and between stage of fibrosis 0–1 versus stage of fibrosis 2–3 hepatitis (**C**).

complex ($r = 0.8805$; 95% CI, 0.7571–0.9432; $p < 0.0001$) was observed with increasing histologic grade, and statistically significant differences were found between all of the grades (Fig. 4). Similarly, levels of both choline-containing compounds ($r = 0.6902$; 95% CI, 0.43–0.8445; $p < 0.0001$) and glutamine–glutamate complex ($r = 0.7291$; 95% CI, 0.4917–0.8656; $p < 0.0001$) consistently varied with degree of steatosis. However, levels of these metabolites had better correlation with histologic grade scores than with degree of steatosis. No separation was achieved between steatosis scores 0 and 1 for choline-containing compounds ($p > 0.05$) or 0 and 1 ($p > 0.05$) or 2 and 3 ($p > 0.05$) for glutamine–glutamate complex (Fig. 5). In contrast, concentration of neither choline-containing compounds ($r = 0.3585$, $p > 0.05$) nor glutamine–glutamate complex ($r = 0.347$, $p > 0.05$) showed any correlation with severity of fibrosis (Fig. 6).

We performed multiple regression analysis to assess whether degree of steatosis or histo-

logic grade made a significant contribution to levels of choline-containing compounds and glutamine–glutamate complex in one patient. As shown in Table 2, after the effect of steatosis was accounted for, histologic grade was the only variable to significantly ($p < 0.0001$) affect the concentrations of choline-containing compounds and glutamine–glutamate complex. Figure 7 shows the [1]H-MR spectra of lipids, choline-containing compounds, and glutamine–glutamate complex from the livers of a control subject and of four typical patients with increasing severity of liver disease.

Histologic Grade Classification Based on Liver Metabolic Profile

The results of classification of histologic grade by means of 10-fold cross-validation stepwise discriminant analysis are shown in Table 3 and Figure 8A. The stepwise discriminant analysis was performed for choline-containing compounds, glutamine–glutamate complex, and lipid. In the first step,

the variable choline-containing compounds had the highest explanatory power. In the second step, the variable glutamine–glutamate complex was combined with choline-containing compounds. The variable lipid was removed from the analysis at the next step with an F value less than the chosen F-to-remove tolerance level (lipid, $F = 0.65$; $p = 0.59$). The cross-validated analysis showed that a correct diagnosis was suggested in six (75%) of eight cases for a histologic grade of 0, in seven (58%) of 12 cases for a grade of 1, in three (60%) of five cases for a grade of 2, and in five of five cases for a grade of 3. The groups with the larger relative misclassification rates were grade 1 (42%) and grade 2 (40%). Among the 12 patients with an actual grade of 1, three patients were classified as having grade 0 disease and two as having grade 2 disease. In two of the five patients with actual grade 2 disease, the disease was incorrectly classified grade 1. Choline-containing compounds had a larger standardized
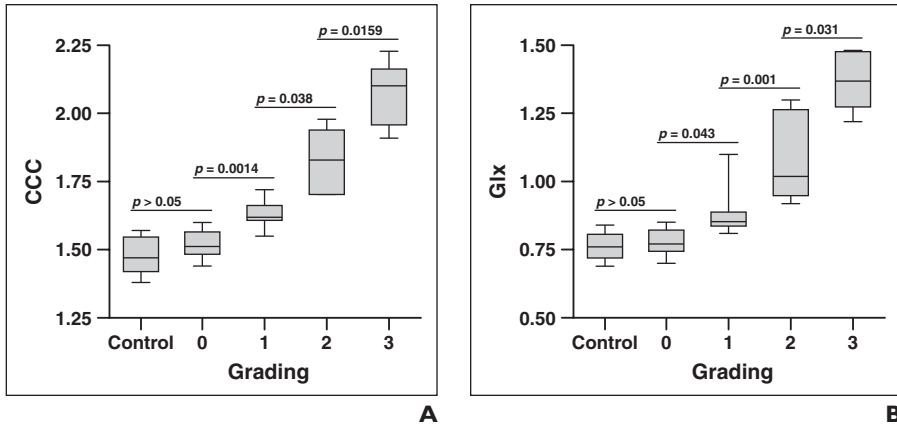
Fig. 4—Correlation between metabolite concentration and histologic grade.
A and **B,** Graphs show elevation of concentration (relative units) of choline-containing compounds (CCC) (**A**) and glutamine–glutamate complex (Glx) (**B**) with increasing grade. Separation between groups is clear.
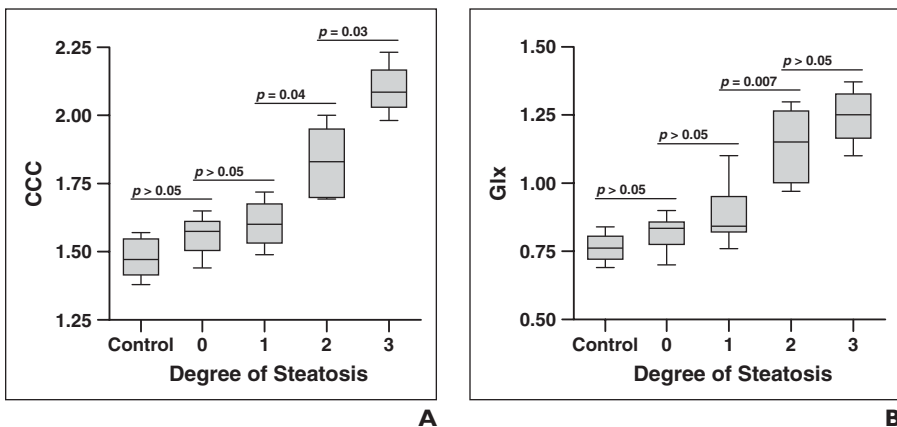

Fig. 5—Correlation between metabolite concentration and degree of steatosis.
A and **B,** Graphs show ratios of concentration (relative units) of choline-containing compounds (CCC) (**A**) and glutamine–glutamate complex (Glx) (**B**) at various steatosis grades. Clear separation between steatosis grade 0–1 and grade 2–3 is shown.
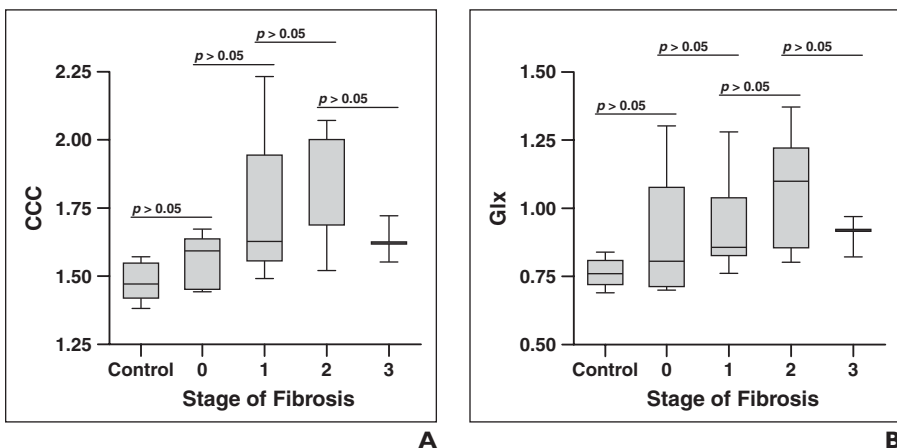

Fig. 6—Correlation between metabolite concentration and stage of fibrosis.
A and **B,** Graphs illustrate ratios of concentration (relative units) of choline-containing compounds (CCC) (**A**) and glutamine–glutamate complex (Glx) (**B**) at various stages of fibrosis. Concentrations of choline-containing compounds and glutamine–glutamate complex showed no correlation with severity of fibrosis.

canonical coefficient (0.70) compared with glutamine–glutamate complex (0.57), accounting for the greatest contribution to discrimination between groups.

Steatosis Classification Based on Liver Metabolic Profile

Results of classification of steatosis by means of 10-fold cross-validated stepwise discriminant analysis are shown in Table 4 and Figure 8B. The stepwise discriminant analysis was performed with all three of the selected variables (choline-containing compounds, glutamine–glutamate complex, and lipid). In the first step, the variable lipid had the highest explanatory power. In the second step, the variable glutamine–glutamate complex was combined with lipid. The variable choline-containing compounds was removed from the analysis at the next step with an F value less than the chosen F-to-remove tolerance level (choline-containing compounds, $F = 2.18$; $p = 0.11$). Cross-validated analysis showed that a correct diagnosis was suggested in nine (75%) of 12 cases for steatosis score 0, in six (66%) of nine cases for steatosis score 1, in four (80%) of five cases for steatosis score 2, and in three (75%) of four cases for steatosis score 3. The group with the larger relative misclassification rate (34%) was steatosis score 1. Among nine patients with an actual steatosis score of 1, two patients were classified as having a score of 0 and one patient as having a score of 2. Lipid played the major role in discriminating between groups, having a larger standardized canonical coefficient (0.82) than glutamine–glutamate complex (0.62).

Discussion

MR spectroscopy is a noninvasive technique that facilitates the study of cellular metabolism. It is a research tool widely used by biochemists for in vitro investigation of pathophysiologic processes and, more recently, by radiologists for in vivo detection of abnormalities. We correlated the in vivo [1]H-MR spectroscopic features of chronic hepatitis C with the histopathologic features of liver biopsy specimens. We found that intrahepatic lipid content measured with [1]H-MR spectroscopy strongly correlates with the degree of steatosis and correlates to a lesser extent with histologic grade and stage of fibrosis determined at histopathologic examination. In addition, in univariate analysis, the [1]H-MR spectroscopic signal intensities of both choline-containing compounds and glutamine–glutamate complex had a direct correlation

TABLE 2: Multiple Regression Results

Variable	t ratio	p	Significance Present	Correlation Matrix[a]
Choline-containing compounds				
Grade of histologic activity	7.994	< 0.0001	Yes	0.9147
Stage of fibrosis	1.327	0.1961	No	0.2216
Degree of steatosis	0.2445	0.8088	No	0.6860
Glutamine–glutamate complex				
Grade of histologic activity	7.153	< 0.0001	Yes	0.8452
Stage of fibrosis	1.759	0.1328	No	0.2835
Degree of steatosis	0.2937	0.7471	No	0.6933

Note—Each p value is the result of comparison of the full model with a simpler model omitting one variable. The procedure is a test of the effect of one variable after the effects of the others are accounted for.
[a]Each correlation coefficient was calculated independently without consideration of the other variables.

with the extent of necroinflammatory activity and steatosis but not with fibrosis stage. In multivariate analysis, the only factor independently associated with levels of choline-containing compounds and glutamine–glutamate complex was necroinflammatory activity.

Since the early 1990s, several groups have reported the utility of [1]H-MR spectroscopy in quantifying fat fraction in tissues [25, 26]. Tarasów et al. [27] performed [1]H-MR spectroscopic examinations to establish normal lipid concentrations in the livers of healthy subjects. Longo et al. [18] and Thomsen et al. [19] found a significant relation between histologic degree of steatosis and lipid content measured with [1]H-MR spectroscopy. Duarte et al. [28], using high-resolution magic angle spinning [1]H-MR spectroscopy for the metabolic assessment of biopsy samples from human liver transplants at the donor and recipient stages, found biochemical differences between livers used for transplants that can be related to the degree and type of lipid composition. We analyzed findings on a cohort of patients with HCV infection with different degrees of steatosis, from none to severe. This stratification and the relatively large sample size assured that subject heterogeneity within groups did not bias our interpretation of the results.

Cho et al. [20] undertook an in vivo study to correlate the in vivo hepatic [1]H-MR spectroscopic features of patients with chronic hepatitis with the histopathologic stages of fibrosis. They reported a decrease in lipid peak that progressed with disease severity, which was evident in stage 4 fibrosis. The discrepancies might have been due to the fact that Cho et al. did not measure absolute lipid peaks and did not correlate the lipid MR spectroscopic measurements with the results of histologic evaluation of steatosis. Moreover, they includ-ed patients with both HCV and hepatitis B virus chronic hepatitis. We, however, did not include patients with cirrhosis, who on clinical and biochemical grounds can be accurately differentiated from subjects in whom cirrhosis has not developed.

Liver steatosis is a frequent histologic finding in patients with chronic hepatitis C, and it has been found to be an important feature of chronic hepatitis C [29, 30]. Whether steatosis is mainly related to host factors or to the virus itself is uncertain. Even when all causes are carefully excluded, a substantial proportion of patients with chronic hepatitis C still have steatosis [31]. In vitro and in vivo studies have shown that HCV core protein can induce steatosis in transfected cells [32] and transgenic mice [33]. It has also been suggested [34] that hepatic steatosis is the morphologic expression of the cytopathic effect of HCV genotype 3. The role of steatosis in the development of fibrosis in patients with chronic hepatitis C continues to be debated. Results of several studies [13–17] have suggested a relation between degrees of liver steatosis and of hepatic fibrosis. In light of these considerations, strict follow-up of steatosis progression in patients with chronic HCV infection, particularly those with genotype 3, is desirable. In this setting, a tool such as [1]H-MR spectroscopy, with which steatosis severity can be evaluated noninvasively, may prove helpful in the management of chronic hepatitis C, for gauging response to treatment, and for correlating the degree of hepatic steatosis with HCV replication in patients with HCV genotype 3.

Hepatosteatosis plays a pivotal pathogenetic role in the development of nonalcoholic steatohepatitis (NASH) [35]. Results of follow-up studies [36–38] with patients with NASH have suggested that progressive liver fibrosis

and cirrhosis develop in 20–40% of these patients. Hydrogen-1 MR spectroscopy, which, as we found, is accurate in evaluation of both fatty infiltration and necroinflammatory activity, can be suggested as a follow-up examination of patients with sonographic evidence of fatty liver and normal serum enzyme levels. We also found that the amount of intrahepatic metabolites, such as choline-containing compounds and glutamine–glutamate complex, increased consistently with histologic grade but not with stage of fibrosis. Cho et al. [20], using [1]H-MR spectroscopy, also found higher levels of these metabolites in a cohort of patients with chronic viral hepatitis than in control subjects. Unlike us, they did find a correlation between concentrations of choline-containing compounds and glutamine–glutamate complex and stage of fibrosis. Cho et al., however, did not stratify patients according to histologic grade but only according to stage of fibrosis. Thus it is possible that patients with high fibrosis scores had also high histologic grade scores. Cho et al. also measured the concentrations of choline-containing compounds and glutamine–glutamate complex with respect to lipid resonance. Because the extent of hepatic steatosis is variable in patients with chronic hepatitis C, quantification of metabolites with respect to lipid resonance may produce spurious results.

Glutamine–glutamate complex is the most abundant free amino acid in the body. It is known to play a regulatory role at the gene and protein levels in several cell-specific processes, including metabolism, cell proliferation, and protein synthesis and degradation [38]. The metabolites that contribute to the choline-containing compound spectroscopic peak (choline, phosphocholine, and glycerophosphorylcholine) are either cell membrane precursors (choline and phosphocholine) or cell membrane degradation products (glycerophosphorylcholine) [39]. Thus the concentration of these substances in tissues is expected to increase with increasing cell turnover. During HCV infection, inflammation due to local compartmentalization of HCV-specific CD4-positive and CD8-positive T cells is responsible for hepatocyte death through apoptosis. As a consequence, the liver attempts to regenerate itself by increasing cell turnover, which is directly related to the degree of inflammation. Moreover, liver-infiltrating T cells have a high proliferation index. It therefore is not surprising that levels of both choline-containing compounds and glutamine–glutamate complex increase with increasing histologic grade. In
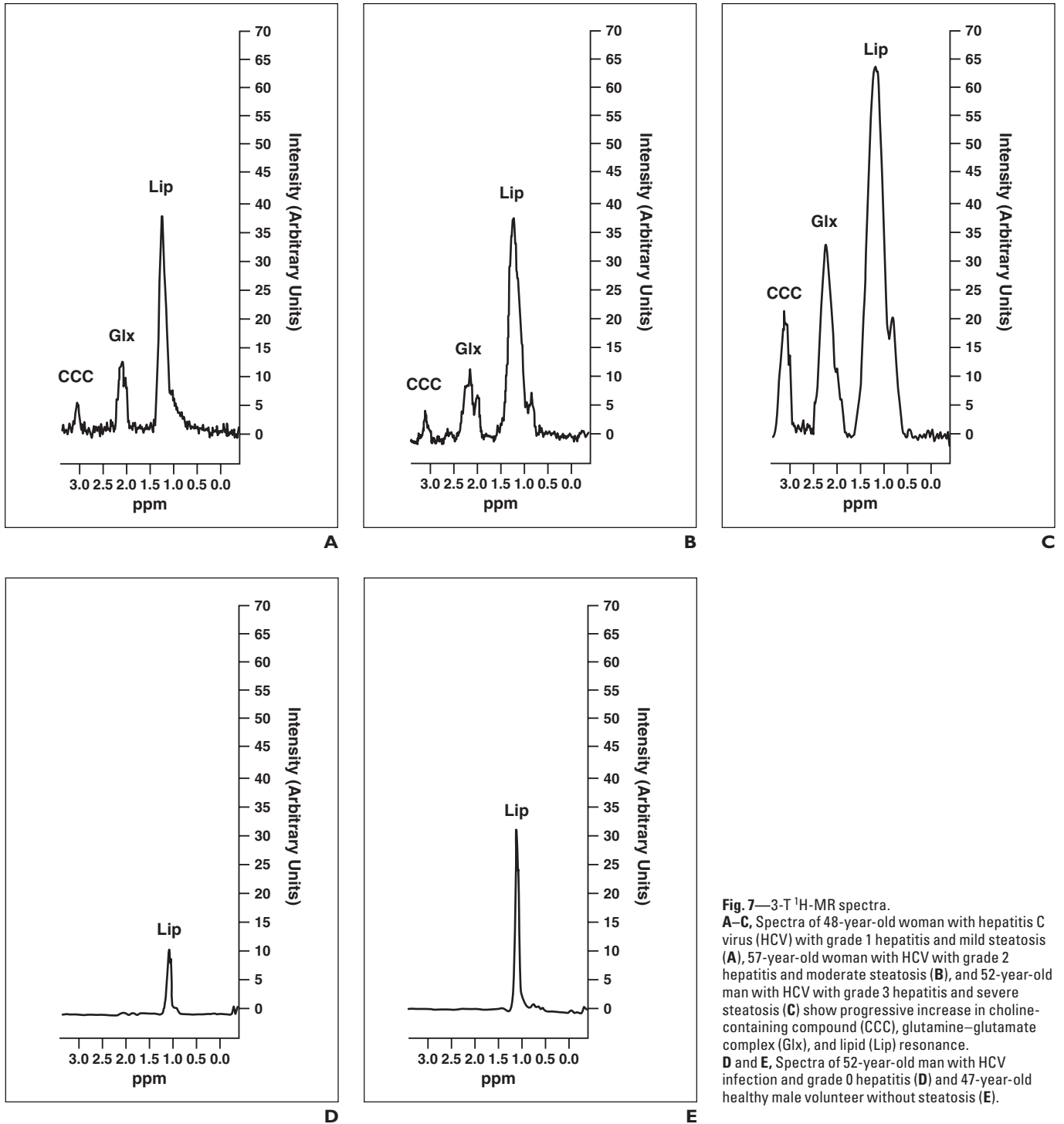
Fig. 7—3-T ^{1}H-MR spectra.
A–C, Spectra of 48-year-old woman with hepatitis C virus (HCV) with grade 1 hepatitis and mild steatosis (**A**), 57-year-old woman with HCV with grade 2 hepatitis and moderate steatosis (**B**), and 52-year-old man with HCV with grade 3 hepatitis and severe steatosis (**C**) show progressive increase in choline-containing compound (CCC), glutamine–glutamate complex (Glx), and lipid (Lip) resonance.
D and **E,** Spectra of 52-year-old man with HCV infection and grade 0 hepatitis (**D**) and 47-year-old healthy male volunteer without steatosis (**E**).

contrast, levels of neither choline-containing compounds nor glutamine–glutamate complex correlate with fibrosis stage. This phenomenon also is not surprising. Fibrosis results from collagen deposition due to activation of stellate cells [14]. Although it is triggered by inflammation and eventually correlates with it, this process may not correlate with fibrosis stage in a single biopsy assessment.

Various methods have been suggested for classification of spectra into groups. We used cross-validated discriminant analysis, a technique that has been widely used in medical science for pattern recognition [40, 41], to assess whether the ^{1}H-MR spectroscopic metabolite patterns we obtained were useful for classifying individual histologic grade and steatosis groups. The results of validated analysis based on choline-containing compound, glutamine–glutamate complex, and lipid resonance were correct in classification

TABLE 3: Classification Count Table for Histologic Grade

Actual Grade	Validated Grade			
	0	1	2	3
0 ($n = 8$)	6 (75)	2	0	0
1 ($n = 12$)	3	7 (58)	2	0
2 ($n = 5$)	0	2	3 (60)	0
3 ($n = 5$)	0	0	0	5 (100)

Note—Results of histologic grade classification by choline, glutamine, and lipid resonances into four grade groups with 10-fold cross-validated stepwise discriminant analysis. Values are number of patients. Values in parentheses are percentage of cases of correct grading according to definitive diagnosis. With the validated model 70% of the groups were correctly classified with a posterior probability greater than 0.70.

TABLE 4: Classification Count Table for Degree of Steatosis

Actual Grade	Validated Grade			
	0	1	2	3
0 ($n = 12$)	9 (75)	3	0	0
1 ($n = 9$)	2	6 (66)	1	0
2 ($n = 5$)	0	1	4 (80)	0
3 ($n = 4$)	0	0	1	3 (75)

Note—Results of steatosis classification by choline, glutamine, and lipid resonances into four steatosis groups with the 10-fold cross-validated stepwise discriminant analysis. Values are number of patients. Values in parentheses are percentage of cases of correct classification according to definitive diagnosis. With the validated model 73% of the groups were correctly classified with a posterior probability greater than 0.70.
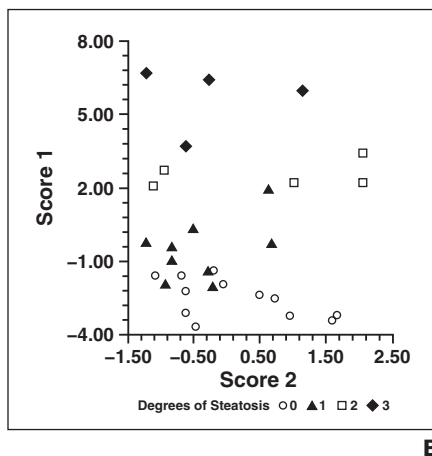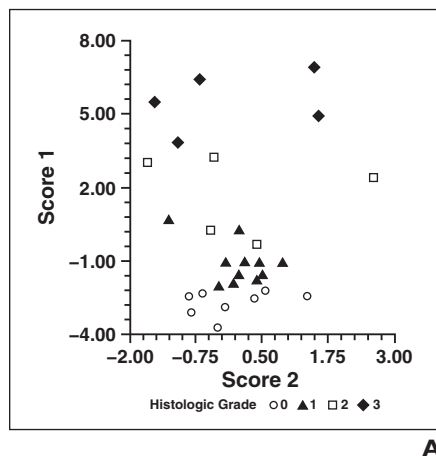
MR spectroscopy is not strictly operator dependent and offers the possibility of performing multiple measurements, reducing intraexamination and interexamination variability. Because the whole sample of tissue included in the VOI is evaluated with MR spectroscopy and the mean spectrum for the entire sample is acquired, a more accurate picture of diffuse hepatic disease is obtained than with histologic characterization of a small tissue sample. In our study, the 10-fold cross-validation method was used to evaluate classification performance. This analysis is generally used when no test sample is available and when the learning sample is too small to have the test sample taken from it, as in our case. To obtain consistent comparative values in our data set, we accepted lower capability to extrapolate our results to as yet unknown data sets.

Although [1]H-MR spectroscopy cannot be used for evaluation of hepatic fibrosis, our data suggest that this technique is a possible alternative to liver biopsy in the evaluation of steatosis and necroinflammatory activity in diffuse liver disease.

Fig. 8—Scatterplots show distribution of complete set of cases by use of two first discriminant functions obtained for linear discriminant analysis: *y*-axis, value obtained with first discriminant function; *x*-axis, value obtained with second discriminant function.
A, Plot shows complete set of cases for grading evaluation. Discriminant function 1 (score 1) has most discriminating power according to its eigenvalue of 9, 32 ($F = 18.5$; $p < 0.001$; Wilks $\Lambda = 0.096$).
B, Plot shows complete set of cases for steatosis evaluation. Discriminant function 1 (score 1) has most discriminating power (eigenvalue, 9, 26; $F = 20.2$; $p < 0.001$; Wilks $\Lambda = 0.085$).

References

1. Pal S, Shuhart MC, Thomassen L, et al. Intrahepatic hepatitis C virus replication correlates with chronic hepatitis C disease severity in vivo. *J Virol* 2006; 80:2280–2290
2. Ngo Y, Munteanu M, Messous D, et al. A prospective analysis of the prognostic value of biomarkers (FibroTest) in patients with chronic hepatitis C. *Clin Chem* 2006; 52:1887–1896
3. Colletta C, Smirne C, Fabris C, et al. Value of two noninvasive methods to detect progression of fibrosis among HCV carriers with normal aminotransferases. *Hepatology* 2005; 42:838–845
4. McGill DB, Rakela J, Zinsmeister AR, Ott BJ. A 21-year experience with major hemorrhage after percutaneous liver biopsy. *Gastroenterology* 1990; 9:1396–1400
5. Cadranel JF, Rufat P, Degos F. Practices of liver biopsy in France: results of a prospective nationwide survey. *Hepatology* 2000; 32:477–481
6. Poynard T, Ratziu V, Bedossa P. Appropriateness of liver biopsy. *Can J Gastroenterol* 2000; 14:543–548
7. Ratziu V, Charlotte F, Heurtier A, et al. Sampling variability of liver biopsy in nonalcoholic fatty liver disease. *Gastroenterology* 2005; 128:1898–1906
8. Younossi ZM, Gramlich T, Liu YC, et al. Nonalcoholic fatty liver disease: assessment of variability in pathologic interpretations. *Mod Pathol* 1998; 11:560–565
9. Kleiner DE, Brunt EM, Van Natta M, et al. Design and validation of a histological scoring system for

of 70% (21 of 30) of the histologic grade groups and 73% (22 of 30) of the steatosis groups. The 21 and 22 correct predictions of grade and steatosis group were associated with a good degree of certainty, evidenced by the associated minimum posterior probability of 0.70 (mean, 0.78 ± 0.07).

A large relative misclassification rate (40%) was observed for histologic grade 3. However, the incorrect predictions (two patients with grade 2 mistaken for grade 1) were associated, respectively, with posterior probabilities of 0.521 and 0.513, whereas the posterior probabilities of grade 2 were, respectively, 0.479 and 0.487. Thus in these two cases, the results of analysis would have been predictive of the correct classifications if a reasonable threshold for

posterior probability had been set. A large misclassification rate also was observed for group 1 of both the histologic grade (42%) and steatosis (34%) classifications, both having an associated posterior probability greater than 0.60 (mean, 0.65 ± 0.4). This result might have been due to the inherent inaccuracy in the standard criterion used for establishing the final diagnosis.

Siddique et al. [42] observed in a cohort of 29 patients with chronic hepatitis C that 44.8% of the subjects had a difference of one or more grades between two biopsy samples from the right lobe. The most commonly observed cause of intrapathologist and interpathologist disagreement is heterogeneous space distribution of disease, such as that observed in the early stages of disease [5, 6].

nonalcoholic fatty liver disease. *Hepatology* 2005; 41:1313–1321

10. Lim AK, Patel N, Hamilton G, Hajnal JV, Golden RD, Taylor-Robinson SD. The relationship of in vivo ^{31}P MR spectroscopy to histology in chronic hepatitis C. *Hepatology* 2003; 37:788–794

11. Angus PW, Dixon RM, Rajagopalan B, et al. A study of patients with alcoholic liver disease by ^{31}P magnetic resonance spectroscopy. *Clin Sci* 1990; 78:33–38

12. Dezortova M, Taimr P, Skoch A, Spicak J, Hajek M. Etiology and functional status of liver cirrhosis by ^{31}P MR spectroscopy. *World J Gastroenterol* 2005; 11:6926–6931

13. Adinolfi LE, Gambardella M, Andreana A, Tripodi MF, Utili R, Ruggiero G. Steatosis accelerates the progression of liver damage of chronic hepatitis C patients and correlates with specific HCV genotype and visceral obesity. *Hepatology* 2001; 33:1358–1364

14. Clouston AD, Jonsson JR, Purdie DM, et al. Steatosis and chronic hepatitis C: analysis of fibrosis and stellate cell activation. *J Hepatol* 2001; 34: 314–320

15. Hourigan LF, Macdonald GA, Purdie D, et al. Fibrosis in chronic hepatitis C correlates significantly with body mass index and steatosis. *Hepatology* 1999; 29:1215–1219

16. Serfaty L, Poujol-Robert A, Carbonell N, Chazouilleres O, Poupon RE, Poupon R. Effect of the interaction between steatosis and alcohol intake on liver fibrosis progression in chronic hepatitis. *Am J Gastroenterol* 2002; 97:1807–1812

17. Castéra L, Hézode C, Roudot-Thoraval F, et al. Worsening of steatosis is an independent factor of fibrosis progression in untreated patients with chronic hepatitis C and paired liver biopsies. *Gut* 2003; 52:288–292

18. Longo R, Ricci C, Masutti F, et al. Fatty infiltration of the liver quantification by 1H localized magnetic resonance spectroscopy and comparison with computed tomography. *Invest Radiol* 1993; 28:297–302

19. Thomsen C, Becker U, Winkler K, Christoffersen P, Jensen M, Henriksen O. Quantification of liver fat using magnetic resonance spectroscopy. *Magn Reson Imaging* 1994; 12:487–495

20. Cho SG, Kim MY, Kim HJ, et al. Chronic hepatitis: in vivo proton MR spectroscopic evaluation of the liver and correlation with histopathologic findings. *Radiology* 2001; 221:740–746

21. Simmonds P, Alberti A, Alter HJ, et al. A proposed system for the nomenclature of hepatitis C viral genotypes. *Hepatology* 1994; 19:1321–1324

22. [No authors listed]. Intraobserver and interobserver variations in liver biopsy interpretation in patients with chronic hepatitis C. The French METAVIR Cooperative Study Group. *Hepatology* 1994; 20:15–20

23. [No authors listed]. Which classification for chronic hepatitis? Lessons from the hepatitis C virus [in French]. *Gastroenterol Clin Biol* 1994; 18:403–406

24. Bell JD, Cox IJ, Sargentoni J, et al. A 31P and 1H-NMR investigation in vitro of normal and abnormal human liver. *Biochim Biophys Acta* 1993; 1225:71–77

25. Cortez-Pinto H, Chatham J, Chacko VP, Arnold C, Rashid A, Diehl AM. Alteration in liver homeostasis in human non-alcoholic steatohepatitis: a pilot study. *JAMA* 1999; 282:1659–1664

26. Chang JS, Taouli B, Salibi N, Hecht EM, Chin DG, Lee VS. Opposed-phase MRI for fat quantification in fat–water phantoms with 1H MR spectroscopy to resolve ambiguity of fat or water dominance. *AJR* 2006; 187:103–106

27. Tarasów E, Siergiejczyk L, Panasiuk A, et al. MR proton spectroscopy in liver examinations of healthy individuals in vivo. *Med Sci Monit* 2002; 8:MT36–MT40

28. Duarte I, Stanley EG, Holmes E, et al. Metabolic assessment of human liver transplants from biopsy samples at the donor and recipient stages using high-resolution magic angle spinning 1H NMR spectroscopy. *Anal Chem* 2005; 77:5570–5578

29. Bach N, Thung SN, Schaffner F. The histological features of chronic hepatitis C and autoimmune chronic hepatitis: a comparative analysis. *Hepatology* 1992; 15:572–577

30. Fischer HP, Willsch E, Bierhoff E, Pfeifer U. Histopathologic findings in chronic hepatitis C. *J Hepatol* 1996; 24:35–42

31. Czaja AJ, Carpenter HA, Santrach PJ, Moore SB. Host- and disease-specific factors affecting ste-

atosis in chronic hepatitis C. *J Hepatol* 1998; 29:198–206

32. Barba G, Harper F, Harada T, et al. Hepatitis C virus core protein shows a cytoplasmic localization and associates to cellular lipid storage droplets. *Proc Natl Acad Sci U S A* 1997; 94:1200–1205

33. Moriya K, Yotsuyanagi H, Shintani Y, et al. Hepatitis C virus core protein induces hepatic steatosis in transgenic mice. *J Gen Virol* 1997; 78:1527–1531

34. Sharma P, Balan V, Hernandez J, et al. Hepatic steatosis in hepatitis C virus genotype 3 infection: does it correlate with body mass index, fibrosis, and HCV risk factors? *Dig Dis Sci* 2004; 49:25–29

35. Lee RG. Nonalcoholic steatohepatitis: a study of 49 patients. *Hum Pathol* 1989; 20:594–599

36. Powell EE, Cooksley GE, Hanson R, Searle J, Halliday RW, Powell LW. The natural history of non-alcoholic steatohepatitis: a follow-up study of 42 patients followed for up to 21 years. *Hepatology* 1990; 11:74–80

37. Okolo PI, Diehl AM. Nonalcoholic steatohepatitis and local fatty liver. In: Feldman M, Scharschmidt BF, Sleisenger MH, eds. *Sleisenger and Fordtran's gastrointestinal and liver disease,* 6th ed. Philadelphia, PA: Saunders, 1988:1215–1220

38. Ochiai H, Higa K, Hishiama N, Hisamatsu S, Fujise H. Characterization of several amino acids transport and glutamine metabolism in MOLT4 human T4 leukemia cells. *Clin Lab Haematol* 2006; 28:399–404

39. Michel V, Yuan Z, Ramsubir S, Bakovic M. Choline transport for phospholipid synthesis. *Exp Biol Med* 2006; 231:490–504

40. François C, Decaestecker C, Petein M, et al. Classification strategies for the grading of renal cell carcinomas, based on nuclear morphometry and densitometry. *J Pathol* 1999; 183:141–150

41. Preul MC, Caramanos Z, Leblanc R, Villemure JG, Arnold DL. Using pattern analysis of in vivo proton MRSI data to improve the diagnosis and surgical management of patients with brain tumors. *NMR Biomed* 1998; 11:192–200

42. Siddique I, El-Naga HA, Madda JP, Memon A, Hasan F. Sampling variability on percutaneous liver biopsy in patients virus infection. *Scand J Gastroenterol* 2003; 38:427–432